European Geothermal Congress 2013
Pisa, Italy, 3-7 June 2013

Effects of sandstone mineralogy and diagenesis on thermal conductivity

Norden, B.[2], Weibel, R. [1], Olivarius, M.[1]

[2] German Research Centre for Geosciences GFZ, Helmholtz Centre Potsdam, Germany.

[1] GEUS, Øster Voldgade 10, 1353 Copenhagen K, Denmark.

ben.norden@gfz-postdam.de

Keywords: Sandstone mineralogy, diagenesis, thermal conductivity.

ABSTRACT

Feasibility studies of geothermal plants typically include modelling of the reservoir conditions, flow rates, thermal properties and expected water temperatures. Though a simplified geological model is used for the modelling; the original variation is known and can be used when performing a risk assessment. Thermal conductivity values applied in the models will typically be average values and the actual variations in the sediments are often not known. With our investigations we add to the knowledge of how the sandstone composition and diagenetic changes affect the thermal conductivity.

Some of the most prominent clastic reservoir rocks for geothermal exploitation onshore Denmark are the Triassic Bunter Sandstone Formation and the Upper Triassic – Lower Jurassic Gassum Formation. The two formations are mineralogically very different. The Bunter Sandstone Formation has an immature mineralogical composition due to limited weathering in the sediment source areas and during deposition in the arid to semi-arid climate. The Gassum Formation is mineralogically more mature due to intensive weathering of the sediments source rocks under the humid climate. Intensive alteration resulting in extensive kaolinite formation also characterise the early diagenesis of the Gassum Formation, except where local early calcite or siderite cement prevail. The Bunter Sandstone Formation is instead characterised by early coatings of iron-oxide/ hydroxide and clay minerals, besides evaporative pore-filling cements as calcite and gypsum (later transformed into anhydrite). The early grain coatings in the Bunter Sandstone Formation inhibit or retard later feldspar and quartz overgrowths; whereas quartz diagenesis can be quite extensive in the Gassum Formation.

Quartz abundance seems to have a direct influence on the rock thermal conductivity. High quartz content and abundant quartz cement typically result in high thermal conductivity, but other minerals, such as for example halite, glauconite and pyrite, may also increase the thermal conductivity. As quartz cement becomes more abundant during burial, there also seems to be a relation to burial depth. With our still ongoing investigations we add to the knowledge of how the sediment composition and diagenesis affect the thermal conductivity, which may improve the risk assessment of geothermal reservoirs.

1. INTRODUCTION

In order to evaluate the temperature field of sedimentary basins, profound knowledge of the subsurface structure, the engaged lithological units and their thermal properties is required. Properties of interest include natural radiogenic heat production of the rock and the rock thermal conductivity. While radiogenic heat production has a second-order effect on the temperature distribution, the thermal conductivity of rock is one of the most important factors that affect the temperature distribution (Blackwell and Steele, 1989). Different thermal conductivities of rocks combined with the subsurface lithological structure may result in a laterally and vertically varying thermal structure even if the heat flow into the basin is regionally the same. In this study we measured the thermal conductivity for the sedimentary rock samples which were investigated for mineralogy, facies environment, and diagenesis with the scope to enable a correlation between mineralogical characteristics and thermal conductivity. This will be used to address the thermal parameterization of geological models of key areas in the Danish Basin.

2. GEOLOGICAL BACKGROUND

Potential geothermal reservoirs onshore Denmark occur in the Mesozoic succession and were deposited in the Norwegian-Danish Basin and the northern margin of the North German Basin. The Norwegian-Danish Basin is bound by shallow basement blocks of the Ringkøbing-Fyn High to the south and the stable Precambrian Baltic Shield to the north (structural highs in Fig. 1) (Vejbæk, 1989). The Mid North Sea High and Ringkøbing-Fyn High, part of which was inundated in the Lower Triassic, separated the Danish Subbasin (eastern part of the Norwegian-Danish Basin) from the North German Basin (Fig. 1; Fisher and Mudge, 1990; Michelsen and Nielsen, 1993). The

isocore maps of the Triassic and Jurassic–Lower Cretaceous successions show a relatively uniform regional thickness in most of the basin except for areas influenced by local faulting and halokinetic movements (Vejbæk, 1989; Britze & Japsen, 1991). Thinning of the Triassic–Lower Jurassic and Upper Jurassic–Lower Cretaceous successions indicates a general shallowing of the basin toward the Ringkø-bing-Fyn High. During Late Cretaceous–Palaeogene times the Sorgenfrei-Tornquist Zone was characterized by inversion and erosion of the Chalk succession (Liboriussen *et al.*, 1987; Michelsen & Nielsen, 1993).

Substantial uplift and erosion occurred during the Neogene along the Northern and eastern basin margins (Japsen et al., 2007).

The Mesozoic reservoir rocks selected for the investigations are the Lower Triassic Bunter Sandstone Formation and the Upper Triassic – Lower Jurassic Gassum Formation due to their fundamental differences in the mineralogical composition. The Bunter Sandstone Formation was deposited in the North German Basin by ephemeral streams, terminal fans or aeolian activity in an arid to semi-arid climate. The thicknesses are up to 300 m (Mathiesen et al., 2009) and present day burial depths vary from 1140–1800 m. The Gassum Formation was deposited in fluvial, paralic and shallow marine environments under humid and vegetated conditions in eastern part of the Norwegian-Danish Basin. It occurs with thicknesses up to 400 m (Mathiesen et al., 2009) and present day burial depths varying from 550–3350 m.

3. METHODS

Measurements of thermal conductivity can be subdivided into direct (laboratory) and indirect (well-logging) approaches (e.g. Blackwell & Steele, 1989; Pribnow & Sass, 1995; Popov et al., 1999, 2003). In this study we used a device based on a transient heat source. The Thermal Conductivity Scanning device (TCS, manufactured by Lippmann and Rauen, GbR) is based on high-resolution optical scanning (Popov et al., 1999). A sample surface is scanned with a focused, movable heat source in combination with two infrared temperature sensors. The error of determination is <3%. A short time of measurement as well as the recording of the thermal-conductivity distribution along a scanning line for each sample are further advantages compared to other methods of thermal conductivity determination. The latter enables also a more detailed study of thermal rock anisotropy, taking into account the heterogeneity of a rock. Therefore, the technique is also of special interest for studying the physical properties of porous sedimentary rocks under dry and fluid-saturated conditions (Popov et al., 2003; Hartmann et al., 2005; Norden & Förster, 2006; Schütz et al., 2012).

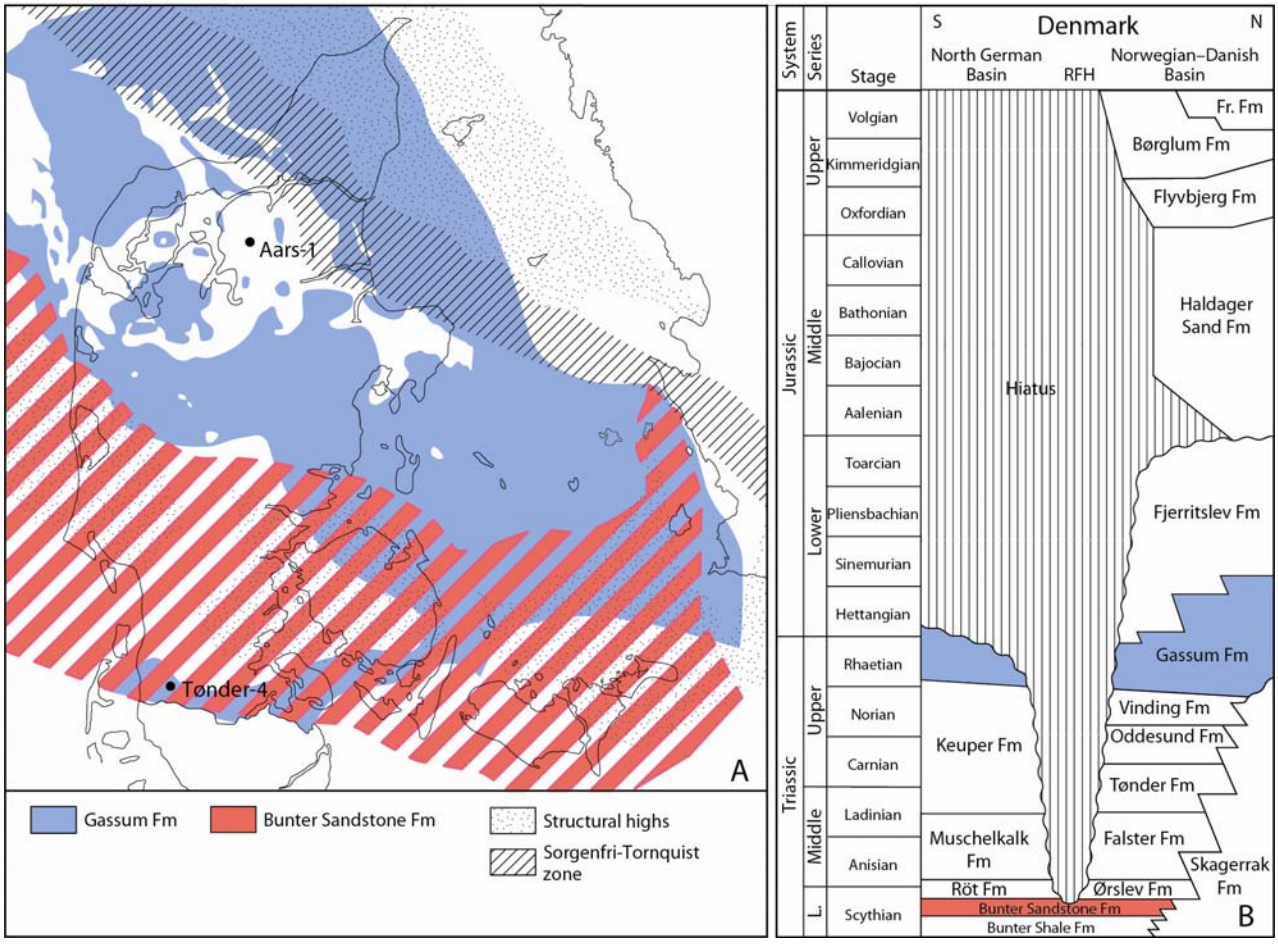

Fig. 1. *Map of Denmark showing the regional potential for geothermal exploitation of the Bunter Sandstone Formation and the Gassum Formation. The distribution of the formations is shown for intervals thicker than 25 m and in the depth interval 800-3000 m. Modified after Anthonsen and Nielsen (2008).*

Measurements were performed on core samples adjacent to core plugs taken for mineralogical and porosity and permeability analyses under ambient room conditions. For a subset of samples, the measurements were carried out also under oven-dried (60°C) and water-saturated conditions. In order to investigate the effect of mineral composition on measured bulk thermal conductivity, the thermal conductivity of the rock matrix was calculated for different lithotypes using the geometric mean model (e.g. Brigaud et al., 1990):

$$\lambda_{geo}=\lambda_{matrix}^{(1-\square)}\cdot\lambda_{pore}^{\square} \quad (1)$$

where λ_{geo} is the thermal conductivity according to the geometric mean; λ_{matrix} is the thermal conductivity of the rock matrix; λ_{pore} is the thermal conductivity of the pore fluid, and ϕ is porosity. Matrix thermal conductivity obtained from measurements was compared with respective values calculated from the major mineral constituents, based on the geometric mean model. In comparison to other mixing law models, the geometric mean equation reproduced the measured values at best. This was recognized also in many other works, e.g. by Midttømme & Roaldset (1998) and latest by Fuchs et al. (2013).

Petrography and mineralogy were evaluated from transmitted light and reflected light microscopy of polished thin sections, which were stained for easy recognition of K-feldspar. Modal compositions of the sandstones were obtained by point counting minimum 500 points in each thin section. Supplementary studies of crystal morphologies, paragenetic relationships and/or chemical composition were performed on gold coated rock chips mounted on stubs and on carbon coated thin sections using a Phillips XL 40 scanning electron microscope (SEM), (with an energy dispersive X-ray analysis (EDX) system. The electron beam was generated by a tungsten filament operating at 17 kV and 50-60 µA.

The porosity and permeability were measured according to the API RP-40 standard (API, 1998). Gas permeability was measured at a confining pressure ~ 2.8 MPa (400 psi), and at a mean N_2 gas pressure of ~ 1.5 bar (bar absolute) = 0.15 MPa (permeabilities below 0.05 mD was measured using a bubble flowmeter). He-porosity was measured unconfined.

4. SANDSTONE MINERALOGY

4.1. Bunter Sandstone Formation

The Bunter Sandstone Formation is characterized by well-sorted, fine-grained, homogeneous, laminated, or small-scale cross-bedded sandstones with occasional thin mudstone intervals.

The sandstones are mainly arkoses and subarkoses (Figs. 2; Fine, 1986; Weibel and Friis, 2004) according to the classification of McBride (1963). The feldspar grains are dominated by K-feldspar and to a lesser extent by Na-rich plagioclase. Rock fragments are characterized by sedimentary rock fragments, especially carbonate clast (Fig. 3), and less abundant igneous and metamorphic rock fragments.

The major authigenic phases are carbonates (calcite and dolomite), anhydrite and clay minerals (. Authigenic calcite occurs in several ways; as overgrowths on ooids or other carbonate rock fragments, as caliche and as poikilotopic cement. Dolomite occurs as pore filling cement and as rhombohedral-shaped crystals commonly inside clay clasts. Anhydrite occurs locally as poikilotopic cement in fluvial sandstones associated with sabkha deposits. Infiltration clays (identified according to Wilson and Pittman, 1977) consist of illite, chlorite and mixed-layer illite/smectite (Weibel and Friis, 2004). Quartz and feldspar overgrowth are common, but volumetrically unimportant. Halite is ubiquitous in samples from the Tønder wells, but it is difficult to determine whether halite was cement in the subsurface or whether it formed as the highly saline pore fluids in the cores dried out. Other accessory authigenic minerals include analcime, red coatings, barite, titanium-oxides and other opaque minerals (Weibel and Friis 2004).

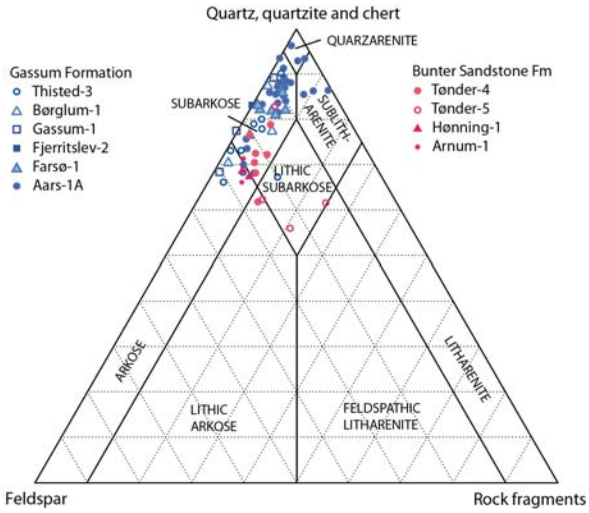

Fig. 2. *Ternary diagram showing the classification, according to McBride (1968), of the Danish Mesozoic onshore sandstones.*

4.2. Gassum Formation

The Gassum Formation comprises fine to medium-grained, well-sorted sand with occasional oversize clay clasts between otherwise subangular to sub-rounded detrital grains.

The sandstones of the Gassum Formation are mainly subarkoses and arkoses (Fig. 2; Friis, 1987) according to the classification by McBride (1963). The framework grains are dominated by monocrystalline quartz, with subordinate polycrystalline quartz. The feldspar grains vary from being common in the northwestern part of the Danish Subbasin to rare in the

eastern part. Plutonic, micaceous metamorphic and sedimentary rock fragments are all rare. Mica, mainly muscovite and subordinate biotite and chlorite, is present in all samples. Organic matter occurs in most samples. Accessory minerals include tourmaline, rutile, zircon and opaque heavy minerals, the latter being dominated by ilmenite intensively altered to leucoxene.

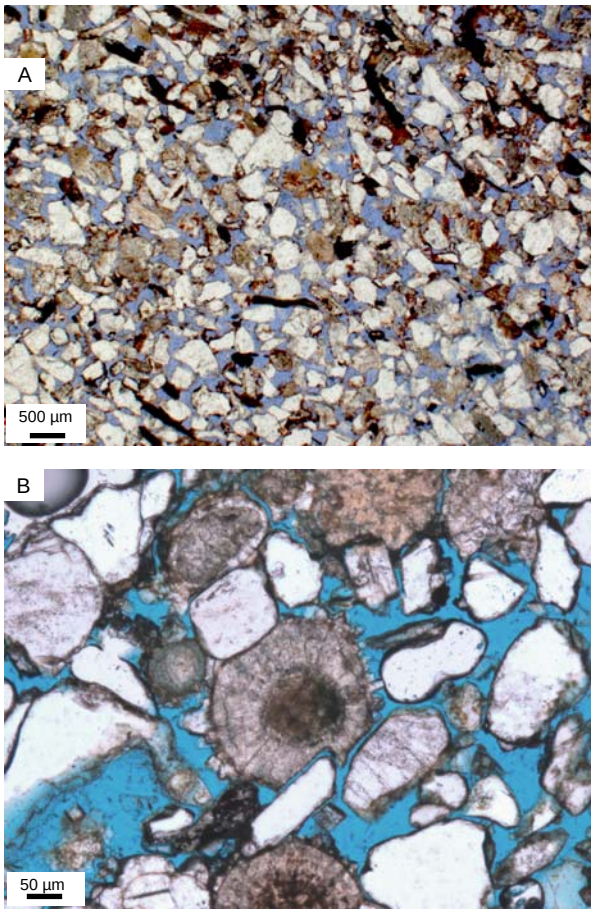

Fig. 3. *A. Overview of sandstone from the Bunter Sandstone Fm. B. Example of ooids and carbonate clasts in the Bunter Sandstone Fm.*

The porosity reduction is mainly due to compaction in sandstones of burial depths down to 1500 m (Friis, 1987); one exception is occasionally extensive siderite precipitation in mica rich samples. Siderite is the first authigenic phase and appears typically as numerous rhombs in the open pore space or between cleavage planes of mica resulting in expansion of the micas original size. Kaolinite typically fills the primary pores close to partly dissolved feldspar grains and more rarely within the intragranular porosity. In deeper buried sandstones quartz diagenesis, carbonate precipitation and feldspar alteration are the major porosity influencing processes. Authigenic quartz is common in most samples. Intense dissolution of quartz grains are found in stylolite zones (Fig. 4). The carbonates (mainly ankerite) can be pervasive in intensely cemented samples or appearing as rhombohedrons (typically calcite and siderite) in sporadic cemented parts. Pore-filling carbonate can be corrosive or replasive towards all other minerals. Volumetrically minor authigenic phases include illite, chlorite, pyrite, albite, K-feldspar and barite.

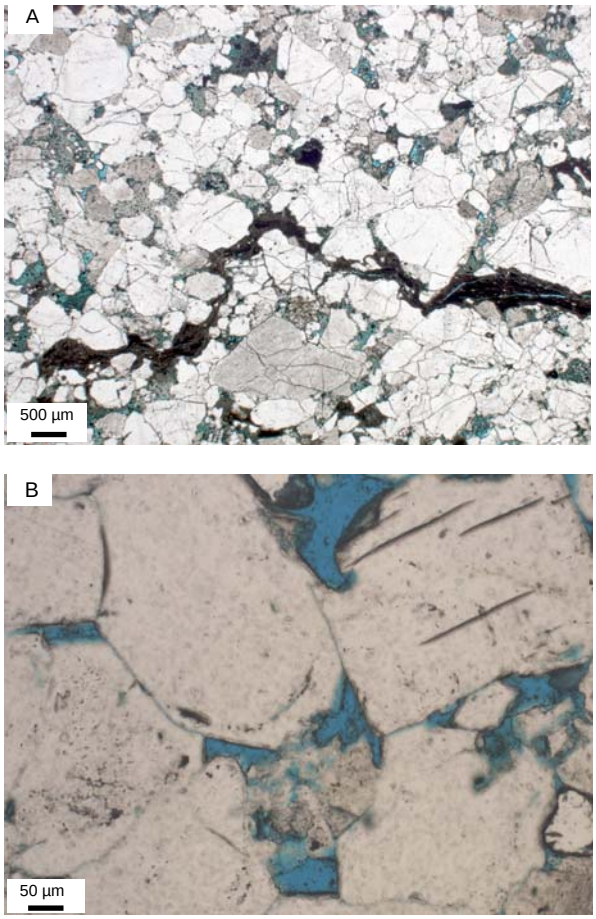

Fig. 4. *A. Overview of sandstone from the Gassum Formation with stylolite forming around mica-rich intevals. B. Example of feldspar overgrowth and quartz overgrowths in the Gassum Formation.*

5. SANDSTONE THERMAL CONDUCTIVITY

5.1 Bunter Sandstone Formation

In total, 42 rock samples of the Bunter Sandstone Formation taken from four different well locations were measured with the TCS device under ambient room conditions and corrected for oven-dried conditions. In addition, the geometric mixing law was applied on the determined TC_D data together with the porosity of the sample, in order to determine the water-saturated thermal conductivity (TC_S) and the porosity-independent matrix thermal conductivity (TC_M). For 27 rock samples, TC_M ranges from 2.9 – 5.0 $Wm^{-1}K^{-1}$, showing a mean value of 3.5 $Wm^{-1}K^{-1}$. For 15 samples, the TC_M seems to be unrealistic high (> 11.8 $Wm^{-1}K^{-1}$). To validate the conducted measurements and to investigate the influence of the mineral composition (and porosity) is investigated in more detail. It turns out that all samples showing an unrealistic high TC_M originate from the Tønder wells, where halite is described to be the ubiquitous present cement. However, it could not be distinguish yet if halite formed from the highly saline pore fluids after

the core was retrieved at the surface and starts to dry out or if halite is already present *in situ*. The thermal conductivity measurements were conducted on larger non-cleaned core samples adjacent to the plugs taken for the porosity determination. Thus, the measurement was performed on a less porous, mainly halite-cemented core surface. In contrast, the plugs taken for the porosity measurements were cleaned prior to the porosity determination. Thus, all halite present was removed and the porosity is significantly higher and may also overestimate the real *in situ* porosity, if halite is present as *in situ* rock cement. If we assume that the pores of the 15 subset samples from the Tønder wells are predominantly cemented with halite, TC_D, TC_S, and TC_M can be recalculated using the adapted new porosity value (lowered by the fraction of the precipitated halite, assumed to amount to 70% of the pore space) and by taking the thermal conductivity of halite (5.2 $Wm^{-1}K^{-1}$, Kopietz et al., 1995) into account. Figure 5 shows the result of the applied correction.

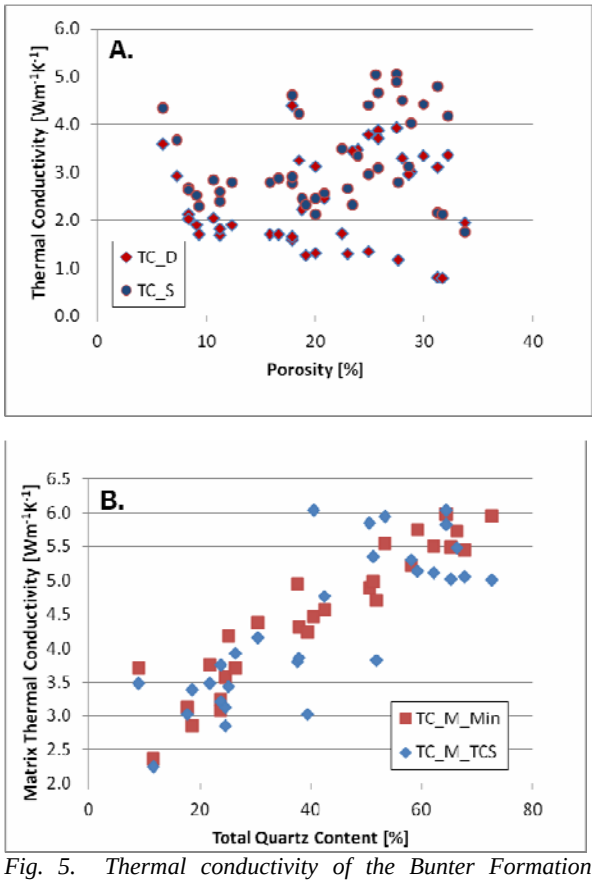

Fig. 5. Thermal conductivity of the Bunter Formation Sandstones: A. Corrected thermal conductivity for oven-dried (TC_D) and saturated (TC_S) conditions. B. Matrix thermal conductivities determined from corrected measurements (TC_M_TCS) and calculated from the mineralogical content (TC_M_Min).

In terms of TC_D and TC_S, there seems to be no correlation to porosity (Fig. 5a). TC_D ranges from 0.8 – 4.4 $Wm^{-1}K^{-1}$ with a mean value of 2.5 $Wm^{-1}K^{-1}$, while the TC_S values are generally higher than the TC_D values (due to the higher thermal conductivity of water, ranging from 1.8 – 5.1 $Wm^{-1}K^{-1}$ with a mean value of 3.3 $Wm^{-1}K^{-1}$). If we plot the determined TC_M against the total Quartz content, a positive correlation of TC_M and the Quartz content (Fig 5b) could be observed. In addition, Figure 5b shows the TC_M calculated based on the thermal conductivity of the main single mineral components, highlighting a fairly good agreement between the measured and the calculated data. The main mineral components and their thermal conductivity are given in Table 1. The mean TC_M based on the mineralogical data amounts to 4.5 $Wm^{-1}K^{-1}$ (range: 2.4 – 6.0 $Wm^{-1}K^{-1}$) which is very similar to the TC_M based on the TCS measurements (mean: 4.4 $Wm^{-1}K^{-1}$, range: 2.3 – 6.0 $Wm^{-1}K^{-1}$).

Mineral / Mineral Assemblage	**TC [$Wm^{-1}K^{-1}$]**	**Reference**
Quartz	7.7	C, H, S
Feldspar-Analcime-Mica	2.3	C, H
Clay (Illite, mixed layers)	1.9	S
Carbonates	3.6	C, H, S
Anhydrite	4.8	C, H
Hematite-Pyrite	12.0	C
Kaolinite	2.6	S
Rock fragments (plutonic)	2.5	N
Organic matter	1.0	S

Table 1. Thermal conductivity (TC) of minerals/mineral associations used in the calculation of the rock matrix thermal conductivity (TC_M).Reference: C: Cermak et al. (1982), H: Horai (1971), S: Schön (1996).

5.2 Gassum Formation

Up to now, 27 samples of the Gassum Formation were analyzed in more detail. Figure 6 shows the first results of the measurements. In contrast to the samples of the Bunter Formation, the thermal conductivity of the samples of the Gassum Formation show a weak trend of decreasing thermal conductivity by increasing porosity for both, TC_D and TC_S (Fig. 6a). TC_D ranges from 0.8 – 3.4 $Wm^{-1}K^{-1}$ with a mean value of 2.4 $Wm^{-1}K^{-1}$, while the TC_S values range from 2.2 – 4.4 $Wm^{-1}K^{-1}$ with a mean value of 3.5 $Wm^{-1}K^{-1}$. The calculated TC_M for the samples analyzed so far do not show exceptionally high values as it was the case for the Tønder wells samples of the Bunter Formation and the plot of TC_M vs. quartz content results in an even stronger positive correlation. The formation of halite was not detected in the samples analyzed so far. The mean TC_M based on the mineralogical data amounts to 4.7 $Wm^{-1}K^{-1}$ (range: 3.8 – 6.5 $Wm^{-1}K^{-1}$) which is in good agreement with TC_M based on the TCS measurements (mean: 4.6 $Wm^{-1}K^{-1}$, range: 3.5 – 5.9 $Wm^{-1}K^{-1}$).

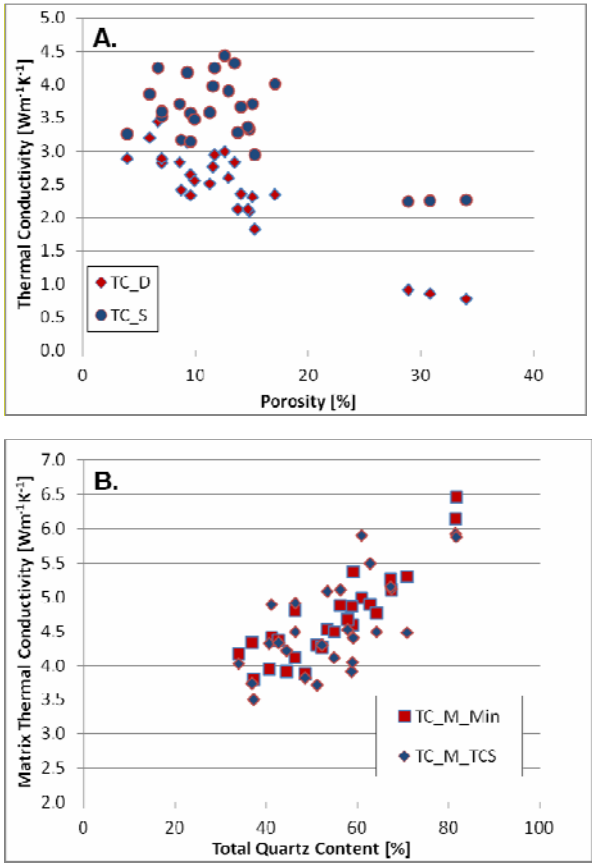

Fig. 6. *Thermal conductivity of the Gassum Formation. Thermal conductivity for oven-dried (TC_D) and saturated (TC_S) conditions. B. Matrix thermal conductivities determined from corrected measurements (TC_M_TCS) and calculated from the mineralogical content (TC_M_Min).*

6. CONCLUSIONS

The Bunter Sandstone and Gassum formations are mineralogically very different. An immature mineralogical composition characterise the Bunter Sandtone Formation due to limited weathering in the sediments source areas and during deposition in the arid to semi-arid climate. A mineralogically more mature composition in the Gassum Formation is the result of intensive weathering of the sediment source rocks under the humid climate and during the early diagenesis. The more mature character of the Gassum Formation (compared to the Bunter Formation) is clearly reflected in the thermal conductivity measurements. The abundance of quartz correlates very strong with the determined matrix thermal conductivity: high quartz content and abundant quartz cement typically result in high thermal conductivity. For the Bunter Formation, this general relation is valid too, but less pronounced. Here, the overall lower quartz content, the retardation of quartz overgrowths and the present of other minerals of high thermal conductivity (e.g. anhydrite and halite) do mask this well-known relationship. As quartz cement becomes more abundant during burial, there also seems to be a relation to burial depth.

The measurements and their interpretations are still ongoing. We will investigate in more detail the relevance of facies and diagenesis on the thermal conductivity. The incorporation of well-log approaches to access thermal conductivity will shed light into the vertical and spatial heterogeneity of this parameter. Further activities will also include the consideration of thermodynamic models to answer the question if halite as cement is present in the subsurface.

REFERENCES

Anthonsen, K. L. and Nielsen, L. H., 2008: COC-02 Assessment of the potential for CO_2 storage in the Norwegian-Danish Basin, International Geological Conference, Oslo, 2008 (Abstract).

API, 1998: API RP40, Recommended practice for core analysis, second edition, American Petroleum Institute, Washington.

Blackwell, D. D. and Steele, J. L., 1989: Thermal conductivity of sedimentary rocks: Measurement and significance, in N. D. Naeser and T. H. McCulloh (eds.) Thermal history of sedimentary basins. New York, Springer, p. 13– 36.

Brigaud, F., Chapman, D.S. and Le Douaran, S., 1990: Estimating thermal conductivity in sedimentary basins using lithological data and geophysical well logs. AAPG Bulletin, 74, 1459–1477.

Britze, P. and Japsen, P., 1991. Geological map of Denmark 1: 400,000. The Danish Basin. "Top Zechstein" of the Triassic (two-way traveltime and depth, thickness and interval velocity). Geological Survey of Denmark Map Series 31. 4 maps and 4 pp.

Čermák, V., Huckenholz, H.-G., Rybach, L., Schmid, R., Schopper, J.R., Schuch, M., Stöffler, D. and Wohlenberg, J., 1982: Physical properties of rocks. In: Angenheister, G. (Ed.), Landolt-Börnstein, vol. 1a, Springer, Heidelberg, pp. 1–373.

Fine, S., 1986: The diagenesis of the Lower Triassic Bunter Sandstone Formation, Onshore Denmark: Geological Survey of Denmark, A 15.

Fisher, M. J. and Mudge, D. C., 1990. Triassic. In: Glennie, K. W. (Ed.), Introduction to the Petroleum Geology of the North Sea, 3rd ed. Blackwell, Oxford, pp. 191 – 218.

Friis, H., 1987: Diagenesis of the Gassum Formation Rhaetian-Lower Jurassic, Danish Subbasin. Geological Survey of Denmark **A 18**, 41pp.

Fuchs, S., Schütz, F., Förster, H.J., Förster, A., 2013: Evaluation of common mixing models for calculating bulk thermal conductivity of sedimentary rocks: Correction charts and new conversion equations. Geothermics, 47, 40–52.

Hartmann, A., Rath, V. and Clauser, C., 2005: Thermal conductivity from core and well log data. International Journal of Rock Mechanics and Mining Sciences, 42, 1042–1055.

Horai, K., 1971: Thermal Conductivity of Rock-Forming Minerals. *J. Geophys. Res.*, 76, 1278–1308.

Japsen, P., Green, P. F., Nielsen, L. H., Rasmussen, E. S. and Bidstrup, T., 2007: Mesozoic–Cenozoic

exhumation events in the eastern North Sea Basin. A multi-disciplinary study based on palaeothermal, palaeoburial, stratigraphic and seismic data. Basin Research 19, 451–490.

Kopietz, J., Greinwald, S., Bochem, M., Mors, K., Czora, C. and Koß, G., 1995: Untersuchungen thermo-physikalischer und elektrischer Eigenschaften von Salzgesteinen, Abschlußbericht 0114283, Bundes-anstalt für Geowissenschaften und Rohstoffe, 29-43.

Liboriussen, J., Ashton, P. and Thygesen, T., 1987: The tectonic evolution of the Fennoscandian Border Zone in Denmark. In: Ziegler, P. A. (ed.), Compressional intra-plate deformations in the Alpine Foreland. Tectonophysics 137, 21-29.

Mathiesen, A., Kristensen, L., Bidstrup, T. and Nielsen, L. H., 2009: Vurdering af det geotermiske potentiale i Danmark. Danmark og Grønlands geologisk undersøgelse Rapport **2009/59**, 30p.

McBride, E. F., 1963: A classification of common sandston-es. Journal of Sedimentary Petrology **33**, 664-669.

Michelsen, O. and Nielsen, L. H., 1993: Structural development of the Fennoscandian Border Zone, offshore Denmark. Marine and Petroleum Geology 10, 124-134.

Midttømme, K. and Roaldset, E., 1998: The effect of grain size on thermal conductivity of quartz sands and silts. *Petroleum Geoscience*, 4, 165–172.

Norden, B. and Förster, A., 2006: Thermal conductivity and radiogenic heat production of sedimentary and magmatic rocks in the Northeast German Basin. *AAPG Bulletin*, 90 (6), 939–962.

Popov, Y.A., Pribnow, D.F.C., Sass, J.H., Williams and C.F. and Burkhardt, H., 1999: Characterization of rock thermal conductivity by high-resolution optical scanning. Geothermics, 28, 253–276.

Popov, Y.A., Tertychnyi, V., Romushkevich, R., Korobkov, D. and Pohl, J, 2003: Interrelations between thermal conductivity and other physical properties of rocks: Experimental data. Pure and Applied Geophysics, 160, 1137–1161.

Pribnow, D. and Sass, J. H., 1995: Determination of thermal conductivity from deep boreholes. Journal of Geophysical Research, 100, 9981–9994.

Schön, J.H., 1996: Physical properties of rocks: fundamentals and principles of petrophysics. In: *Handbook of Geophysical Exploration* (Ed. by K. Helbig and S. Teitel), pp. 323-373, Section 8, Thermal Properties of Rocks, Oxford, United Kingdom, Pergamon, 18.

Schütz, F., Norden, B. and Förster, A., 2012: Thermal properties of sediments in southern Israel: a comprehensive data set for heat flow and geothermal energy studies. Basin Research, 24 (3), 357–376. DOI: 10.1111/j.1365-2117.2011.00529.

Vejbæk, O. 1989: Effects of asthenospheric heat flow in basin modeling exemplified with the Danish Basin. Earth and Planetary Science Letters 95, 97-114.

Weibel, R. and Friis, H., 2004: Opaque minerals as keys for distinguishing oxidising and reducing diagenetic conditions in the Lower Triassic Bunter Sandstone, North German Basin. Sedimentary Gelogy **169**, 129–149.

Wilson, M. D. and Pittman, E. D., 1977. Authigenic clays in sandstones: recognition and influence on reservoir properties and paleoenvironmental analysis. Journal of Sedimentary Petrology 47, 3 – 31.

Acknowledgements

This contribution is published with the permission of the Geological Survey of Denmark and Greenland and is an outcome of the project "The geothermal energy potential in Denmark - reservoir properties, temperature distribution and models for utilisation" under the program Sustainable Energy and Environment funded by the Danish Agency for Science, Technology and Innovation.